

Origin of large thermal effect in the Casimir interaction between two graphene sheets

G. L. Klimchitskaya^{1,2} and V. M. Mostepanenko^{1,2}

¹*Central Astronomical Observatory at Pulkovo of the Russian Academy of Sciences, St.Petersburg, 196140, Russia*

²*Institute of Physics, Nanotechnology and Telecommunications, St.Petersburg State Polytechnical University, St.Petersburg, 195251, Russia*

Abstract

Using the recently derived representation for the polarization tensor in (2+1)-dimensional space-time allowing an analytic continuation to the entire plane of complex frequencies, we obtain simple analytic expressions for the reflection coefficients of graphene at nonzero Matsubara frequencies. In the framework of the Lifshitz theory, these coefficients are shown to lead to nearly exact results for the Casimir free energy and pressure between two graphene sheets. The constituent parts of large thermal effect, arising in the Casimir interaction at short separations due to an explicit parametric dependence of the polarization tensor on the temperature and an implicit dependence through a summation over the Matsubara frequencies, are calculated. It is demonstrated that an explicit thermal effect exceeds an implicit one at shorter separations, both effects are similar in magnitudes at moderate separations, and that an implicit effect becomes a larger one with further increase of separation. Possible applications of the developed formalism, other than the Casimir effect, are discussed.

PACS numbers: 78.67.Wj, 42.50.Lc, 65.80.Ck, 12.20.-m

I. INTRODUCTION

Graphene has already assumed great importance as a material possessing unusual mechanical, electrical and optical properties of high promise for various applications [1]. These properties are due to 2D character of graphene. In contrast to standard 3D materials, quasi-particles in pristine (undoped) graphene are massless Dirac fermions which possess the linear dispersion relation but move with the Fermi velocity rather than with the velocity of light [1, 2]. Taking into account that graphene is considered as a potential element of micro- and nanoelectromechanical devices, much attention is attracted to forces acting between two graphene sheets and between a graphene sheet and some element made of an ordinary material (metallic, dielectric or semiconductor). These forces are caused by the zero-point and thermal fluctuations of the electromagnetic field and are called the *van der Waals* or *Casimir forces* depending on the range of separations considered [3, 4]. The fluctuation induced forces are known also under the generic name of *dispersion forces*.

The van der Waals and Casimir forces acting between two graphene sheets and between a graphene sheet and a 3D material were studied theoretically by many authors in the framework of various approaches (see, for instance, Refs. [5–15]). The most important breakthrough was made in Ref. [8], where it was shown that for graphene the thermal effect in the Casimir force becomes crucial at by an order of magnitude shorter separations than for ordinary materials. This result was obtained using the longitudinal density-density correlation function in the random-phase approximation, and the relativistic effects were shown to be not essential.

The most straightforward description of the van der Waals and Casimir forces in layered systems including graphene is given by the Lifshitz theory [3, 4, 16] with reflection coefficients expressed via the polarization tensor of graphene in (2+1)-dimensional space-time. The explicit analytic expressions for the components of this tensor were obtained in Refs. [17, 18] at zero and nonzero temperature, respectively. Using the values of the polarization tensor of graphene at the imaginary Matsubara frequencies, a lot of numerical computations of the Casimir and Casimir-Polder forces between graphene and different materials and atoms has been performed [17–27]. The formalisms exploiting the polarization tensor and the density-density correlation function have been compared [28]. It was shown [28] that these formalisms are equivalent if one uses the exact temperature-dependent longitudinal and

transverse density-density correlation functions. Computations using the polarization tensor confirmed the existence of large thermal effect in the Casimir interaction of graphene sheets at short separations, as predicted in Ref. [8]. Furthermore, the results computed using the polarization tensor of graphene at nonzero temperature [29, 30] were found to be in very good agreement with first measurement of the gradient of the Casimir force between a Au-coated sphere and a graphene-coated substrate by means of a dynamic atomic force microscope [31]. The computational results obtained using the hydrodynamic model of graphene [6, 7, 11, 26] were shown to be excluded by the measurement data over a wide range of separations [32].

In this paper, we investigate an origin of the large thermal effect in the interaction of two graphene sheets at short separations from a few nanometers to a few hundred nanometers. Our aim is to determine the relative contributions to the Casimir free energy and pressure due to an explicit dependence of the polarization tensor on the temperature as a parameter and an implicit dependence on the temperature through a summation over the Matsubara frequencies. For this purpose, we circumvent cumbersome computations using the exact expressions for the polarization tensor and find a transparent way of performing simple analytic calculations in powers of a natural small parameter as far as possible. It is significant that the polarization tensor of graphene at nonzero temperature obtained in Ref. [18] is not well adapted for analytic calculations. The point is that it is valid only at the discrete imaginary Matsubara frequencies and its immediate continuation to the entire imaginary frequency axis does not satisfy necessary physical conditions [33]. Another form of the polarization tensor of graphene, valid over the whole plane of complex frequency, including the imaginary and real frequency axes, was found in Ref. [33]. At the imaginary Matsubara frequencies the polarization tensor of Ref. [33] takes the same values as the one of Ref. [18], but presents better opportunities for analytic calculations due to much simpler mathematical structure.

Here, we use the polarization tensor in the representation of Ref. [33] and obtain simple asymptotic expressions for both the thermal correction to this tensor and for the reflection coefficients of the electromagnetic oscillations from a graphene sheet at the Matsubara frequencies. The developed formalism is applied to calculate the Casimir free energy and pressure between two graphene sheets at room temperature. We compare our results with previously made [22] numerical computations using exact expressions for the polarization tensor in the representation of Ref. [18]. We demonstrate that the error of our asymptotic

results is only a small fraction of a percent over the whole region of physically meaningful values of parameters. Then we investigate the origin of large thermal effect at short separations. It is shown that the explicit and implicit contributions to the dependencies of the Casimir free energy and pressure of graphene on the temperature are equally important parts of the large thermal effect. In so doing, the major contribution to the thermal effect due to an explicit temperature dependence of the polarization tensor originates from the zero-frequency Matsubara term.

The structure of the paper is the following. In Sec. II we introduce the main notations, formulate our perturbation approach and obtain simple asymptotic expressions for the polarization tensor of graphene and reflection coefficients. Section III is devoted to the investigation of large thermal effect in the Casimir free energy of two parallel graphene sheets. In Sec. IV the same is done for the Casimir pressure. Section V contains our conclusions and discussion.

II. SIMPLE ASYMPTOTIC EXPRESSIONS FOR THE POLARIZATION TENSOR OF GRAPHENE AND REFLECTION COEFFICIENTS

In the framework of the Dirac model, the reflection coefficients of the electromagnetic oscillations from graphene can be expressed via the polarization tensor of graphene in (2+1)-dimensional space-time. To calculate the Casimir free energy and pressure between two graphene sheets one needs the reflection coefficients calculated at the pure imaginary Matsubara frequencies [18, 20, 22]

$$\begin{aligned} r_{\text{TM}}(i\xi_l, k_{\perp}) &= \frac{q_l \Pi_{00}(i\xi_l, k_{\perp})}{q_l \Pi_{00}(i\xi_l, k_{\perp}) + 2\hbar k_{\perp}^2}, \\ r_{\text{TE}}(i\xi_l, k_{\perp}) &= -\frac{\Pi(i\xi_l, k_{\perp})}{\Pi(i\xi_l, k_{\perp}) + 2\hbar k_{\perp}^2 q_l} \end{aligned} \quad (1)$$

for two independent polarizations of the electromagnetic field, transverse magnetic (TM) and transverse electric (TE). Here, $\xi_l = 2\pi k_B T l / \hbar$, where k_B is the Boltzmann constant, T is the temperature and $l = 0, 1, 2, \dots$, are the Matsubara frequencies, k_{\perp} is the magnitude of the projection of the photon wave vector on the plane of graphene, $q_l = (k_{\perp}^2 + \xi_l^2 / c^2)^{1/2}$, Π_{mn} with $m, n = 0, 1, 2$ are the components of the polarization tensor of graphene in (2+1)-dimensional space-time, and the quantity Π is defined as

$$\Pi(i\xi_l, k_{\perp}) = k_{\perp}^2 \Pi_{\text{tr}}(i\xi_l, k_{\perp}) - q_l^2 \Pi_{00}(i\xi_l, k_{\perp}), \quad (2)$$

where $\Pi_{\text{tr}} \equiv \Pi_m^m$. Note that the reflection coefficients (1) can be equivalently rewritten via the longitudinal and transverse density-density correlation functions, or conductivities, or polarizabilities or nonlocal dielectric permittivities of graphene [28].

The components of the polarization tensor of graphene at temperature T can be presented in the form

$$\begin{aligned}\Pi_{00}(i\xi_l, k_\perp) &= \Pi_{00}^{(0)}(i\xi_l, k_\perp) + \Delta_T \Pi_{00}(i\xi_l, k_\perp), \\ \Pi(i\xi_l, k_\perp) &= \Pi^{(0)}(i\xi_l, k_\perp) + \Delta_T \Pi(i\xi_l, k_\perp),\end{aligned}\quad (3)$$

where $\Pi_{00}^{(0)}$, $\Pi^{(0)}$ are the respective quantities calculated at zero temperature, but with continuous frequencies ξ replaced by the Matsubara frequencies ξ_l , and $\Delta_T \Pi_{00}$, $\Delta_T \Pi$ are the thermal corrections to them.

For a pristine (gapless) graphene under consideration in this paper, the components of the polarization tensor at $T = 0$ K take especially simple form [17]

$$\Pi_{00}^{(0)}(i\xi_l, k_\perp) = \frac{\pi\alpha\hbar k_\perp^2}{\tilde{q}_l}, \quad \Pi^{(0)}(i\xi_l, k_\perp) = \pi\alpha\hbar k_\perp^2 \tilde{q}_l, \quad (4)$$

where $\alpha = e^2/(\hbar c) \approx 1/137$ in the fine-structure constant,

$$\tilde{q}_l = \left(\frac{v_F^2}{c^2} k_\perp^2 + \frac{\xi_l^2}{c^2} \right)^{1/2} \quad (5)$$

and $v_F \approx c/300$ is the Fermi velocity. The respective reflection coefficients (1) are given by

$$r_{\text{TM}}^{(0)}(i\xi_l, k_\perp) = \frac{\pi\alpha q_l}{\pi\alpha q_l + 2\tilde{q}_l}, \quad r_{\text{TE}}^{(0)}(i\xi_l, k_\perp) = -\frac{\pi\alpha\tilde{q}_l}{\pi\alpha\tilde{q}_l + 2q_l}. \quad (6)$$

For the thermal corrections to the polarization tensor we use the expressions obtained in Ref. [33]

$$\begin{aligned}\Delta_T \Pi_{00}(i\xi_l, k_\perp) &= \frac{16\alpha\hbar c^2}{v_F^2} \int_0^\infty \frac{dq_\perp}{e^{\hbar c q_\perp / (k_B T)} + 1} \\ &\times \left[1 - \frac{1}{\tilde{q}_l} \text{Re} W(\xi_l, k_\perp, q_\perp) \right], \\ \Delta_T \Pi(i\xi_l, k_\perp) &= \frac{16\alpha\hbar c^2}{v_F^2} \int_0^\infty \frac{dq_\perp}{e^{\hbar c q_\perp / (k_B T)} + 1} \\ &\times \left\{ -\frac{\xi_l^2}{c^2} + \tilde{q}_l \left[\text{Re} W(\xi_l, k_\perp, q_\perp) - \frac{v_F^2 k_\perp^2}{c^2} \text{Re} \frac{1}{W(\xi_l, k_\perp, q_\perp)} \right] \right\}.\end{aligned}\quad (7)$$

Here, the integration is performed over the magnitude of a two-dimensional wave vector of the electronic excitation and the quantity W is defined as

$$W(\xi_l, k_\perp, q_\perp) = \left(\tilde{q}_l^2 - 4q_\perp^2 + \frac{4i\xi_l q_\perp}{c} \right)^{1/2}. \quad (8)$$

The expressions in Eq. (7) have the same values as the respective more complicated expressions in Ref. [18], but, in contrast to the latter, can be immediately analytically continued to the whole plane of complex frequency.

It is possible to simplify Eq. (7) taking into account that

$$\begin{aligned} \text{Re}W(\xi_l, k_\perp, q_\perp) &= \frac{1}{\sqrt{2}} \left[\sqrt{(\tilde{q}_l^2 - 4q_\perp^2)^2 + \frac{16\xi_l^2 q_\perp^2}{c^2}} + \tilde{q}_l^2 - 4q_\perp^2 \right]^{1/2}, \\ \text{Re} \frac{1}{W(\xi_l, k_\perp, q_\perp)} &= \frac{\text{Re}W(\xi_l, k_\perp, q_\perp)}{\sqrt{(\tilde{q}_l^2 - 4q_\perp^2)^2 + \frac{16\xi_l^2 q_\perp^2}{c^2}}}. \end{aligned} \quad (9)$$

Using Eqs. (5) and (9) and introducing the new integration variable $u = 2q_\perp/\tilde{q}_l$, we rewrite Eq. (7) in the form

$$\begin{aligned} \Delta_T \Pi_{00}(i\xi_l, k_\perp) &= \frac{8\alpha\hbar c^2 \tilde{q}_l}{v_F^2} \int_0^\infty \frac{du}{e^{B_l u} + 1} \\ &\times \left\{ 1 - \frac{1}{\sqrt{2}} \left[\sqrt{(1+u^2)^2 - 4\frac{v_F^2 k_\perp^2 u^2}{c^2 \tilde{q}_l^2}} + 1 - u^2 \right]^{1/2} \right\}, \\ \Delta_T \Pi(i\xi_l, k_\perp) &= \frac{8\alpha\hbar c^2 \tilde{q}_l}{v_F^2} \int_0^\infty \frac{du}{e^{B_l u} + 1} \\ &\times \left\{ -\frac{\xi_l^2}{c^2} + \frac{\tilde{q}_l^2}{\sqrt{2}} \left[\sqrt{(1+u^2)^2 - 4\frac{v_F^2 k_\perp^2 u^2}{c^2 \tilde{q}_l^2}} + 1 - u^2 \right]^{1/2} \right. \\ &\times \left. \left[1 - \frac{v_F^2 k_\perp^2}{c^2 \tilde{q}_l^2 \sqrt{(1+u^2)^2 - 4\frac{v_F^2 k_\perp^2 u^2}{c^2 \tilde{q}_l^2}}} \right] \right\}, \end{aligned} \quad (10)$$

where $B_l \equiv \hbar c \tilde{q}_l / (2k_B T)$.

Now we consider approximate expressions for the quantities (10) applicable at any $l \geq 1$ for calculations of the Casimir force using the Lifshitz formula. For this purpose we note that at room temperature $T = 300$ K the first Matsubara frequency $\xi_1 \approx 2.4 \times 10^{14}$ rad/s. Taking into account that the characteristic photon wave vector giving the major contribution into the Casimir free energy and pressure is equal to $k_\perp = 1/(2a)$, where a is the separation distance between the plates [4, 34], one concludes that the natural parameter entering Eq. (10) can be considered as a small one at all separations $a \geq 10$ nm,

$$\frac{4v_F^2 k_\perp^2}{c^2 \tilde{q}_l^2} < \frac{4v_F^2 k_\perp^2}{c^2 \tilde{q}_1^2} \ll 1. \quad (11)$$

Thus, at $a = 10$ nm this parameter is less than 0.17, at $a = 20$ nm less than 0.04 and further decreases with increase of separation.

Now we expand the square roots in Eq. (10) in powers of the small parameter (11) and preserve only the zero and first order contributions. Furthermore, from Eq. (11) we have $v_F^2 k_\perp^2 \ll \xi_1^2$ and, thus, $B_l \approx \hbar \xi_l / (2k_B T) = \pi l$. Then from Eq. (10) one obtains

$$\begin{aligned}\Delta_T \Pi_{00}(i\xi_l, k_\perp) &= \frac{\alpha \hbar k_\perp^2}{\tilde{q}_l} Y_l, \\ \Delta_T \Pi(i\xi_l, k_\perp) &= \alpha \hbar k_\perp^2 \tilde{q}_l Y_l,\end{aligned}\tag{12}$$

where we have introduced the notation

$$Y_l = 4 \int_0^\infty \frac{du}{e^{\pi l u} + 1} \frac{u^2}{1 + u^2}.\tag{13}$$

By combining Eqs. (4) and (12) in accordance with Eq. (3), we arrive to the following simple asymptotic expressions for the polarization tensor of graphene

$$\begin{aligned}\Pi_{00}(i\xi_l, k_\perp) &= \frac{\alpha \hbar k_\perp^2}{\tilde{q}_l} (\pi + Y_l), \\ \Pi(i\xi_l, k_\perp) &= \alpha \hbar k_\perp^2 \tilde{q}_l (\pi + Y_l).\end{aligned}\tag{14}$$

Substituting Eq. (14) in Eq. (1), one obtains simple equations for the reflection coefficients

$$\begin{aligned}r_{\text{TM}}(i\xi_l, k_\perp) &= \frac{\alpha q_l (\pi + Y_l)}{\alpha q_l (\pi + Y_l) + 2\tilde{q}_l}, \\ r_{\text{TE}}(i\xi_l, k_\perp) &= -\frac{\alpha \tilde{q}_l (\pi + Y_l)}{\alpha \tilde{q}_l (\pi + Y_l) + 2q_l}.\end{aligned}\tag{15}$$

As can be seen in Eqs. (14) and (15), in both the polarization tensor and reflection coefficients the relative contribution of each term with $l \geq 1$ is characterized by the ratio Y_l/π . In this connection it is instructive that for $l = 1, 2, 3, 4,$ and 5 the quantity Y_l/π is equal to $0.041, 0.0074, 0.0024, 0.0011,$ and 5.5×10^{-4} , respectively, and further decreases with increasing l .

Recall that Eqs. (14) and (15) are valid under a condition $l \geq 1$. For $l = 0$ the thermal correction to Π_{00} can be obtained from the first formula in Eq. (10)

$$\Delta_T \Pi_{00}(0, k_\perp) = \frac{16\alpha c}{v_F^2} \left(k_B T \ln 2 - \frac{\hbar v_F k_\perp}{2} \int_0^1 \frac{du}{e^{B_0 u} + 1} \sqrt{1 - u^2} \right),\tag{16}$$

where $B_0 = \hbar v_F k_\perp / (2k_B T)$. In the derivation of Eq. (16) we have taken into account that

$$\sqrt{(1 - u^2)^2} = \begin{cases} 1 - u^2, & u \leq 1, \\ u^2 - 1, & u > 1. \end{cases}\tag{17}$$

Using the first formula in Eq. (4), from Eqs. (1), (3) and (16) we obtain

$$r_{\text{TM}}(0, k_{\perp}) = \frac{\alpha c \{16k_B T \ln 2 + \hbar k_{\perp} v_F [\pi - 8X(k_{\perp})]\}}{\alpha c \{16k_B T \ln 2 + \hbar k_{\perp} v_F [\pi - 8X(k_{\perp})]\} + 2\hbar k_{\perp} v_F^2}, \quad (18)$$

where

$$X(k_{\perp}) \equiv \int_0^1 \frac{du}{e^{B_0 u} + 1} \sqrt{1 - u^2}. \quad (19)$$

Equation (18) is an exact one. It can be rewritten in an equivalent form

$$r_{\text{TM}}(0, k_{\perp}) = 1 - \frac{2\hbar k_{\perp} v_F^2}{\alpha c \{16k_B T \ln 2 + \hbar k_{\perp} v_F [\pi - 8X(k_{\perp})]\} + 2\hbar k_{\perp} v_F^2}. \quad (20)$$

From Eq. (20) it is seen that at zero Matsubara frequency the values of the TM reflection coefficient are rather close to unity and

$$\lim_{k_{\perp} \rightarrow 0} r_{\text{TM}}(0, k_{\perp}) = 1. \quad (21)$$

In a similar way, for $l = 0$ the thermal correction to Π can be found from the second formula in Eq. (10)

$$\Delta_T \Pi(0, k_{\perp}) = -\frac{8\alpha \hbar v_F k_{\perp}^3}{c} Z(k_{\perp}), \quad (22)$$

where

$$Z(k_{\perp}) \equiv \int_0^1 \frac{du}{e^{B_0 u} + 1} \frac{u^2}{\sqrt{1 - u^2}}. \quad (23)$$

Using the second formula in Eq. (4), from Eqs. (1), (3) and (22) one obtains

$$r_{\text{TE}}(0, k_{\perp}) = -\frac{\alpha v_F [\pi - 8Z(k_{\perp})]}{\alpha v_F [\pi - 8Z(k_{\perp})] + 2c}. \quad (24)$$

It is easily seen that

$$|r_{\text{TE}}(0, k_{\perp})| < \frac{\alpha \pi v_F}{2c} \approx 3.8 \times 10^{-5} \quad (25)$$

and, thus, the TE mode does not contribute into the classical limit [23, 24].

III. INVESTIGATION OF THE THERMAL EFFECT FOR THE CASIMIR FREE ENERGY

The Casimir free energy per unit area of two parallel graphene sheets separated by a distance a at temperature T in thermal equilibrium with an environment is given by the Lifshitz formula [3, 4, 16]

$$\begin{aligned} \mathcal{F}(a, T) = & \frac{k_B T}{2\pi} \sum_{l=0}^{\infty} \int_0^{\infty} k_{\perp} dk_{\perp} \{ \ln[1 - r_{\text{TM}}^2(i\xi_l, k_{\perp}) e^{-2aq_l}] \\ & + \ln[1 - r_{\text{TE}}^2(i\xi_l, k_{\perp}) e^{-2aq_l}] \}, \end{aligned} \quad (26)$$

where the prime on the summation sign indicates that the term with $l = 0$ is divided by two and the reflection coefficients are given in Eq. (1).

For convenience in numerical computations we rewrite Eq. (26) in terms of dimensionless variables

$$y = 2qla, \quad \zeta_l = \frac{2a\xi_l}{c}. \quad (27)$$

Then the Casimir free energy takes the form

$$\begin{aligned} \mathcal{F}(a, T) = & \frac{k_B T}{8\pi a^2} \sum_{l=0}^{\infty} ' \int_{\zeta_l}^{\infty} y dy \{ \ln[1 - r_{\text{TM}}^2(i\zeta_l, y)e^{-y}] \\ & + \ln[1 - r_{\text{TE}}^2(i\zeta_l, y)e^{-y}] \}, \end{aligned} \quad (28)$$

where the reflection coefficients are

$$\begin{aligned} r_{\text{TM}}(i\zeta_l, y) &= \frac{y\tilde{\Pi}_{00}(i\zeta_l, y)}{y\tilde{\Pi}_{00}(i\zeta_l, y) + 2(y^2 - \zeta_l^2)}, \\ r_{\text{TE}}(i\zeta_l, y) &= -\frac{\tilde{\Pi}(i\zeta_l, y)}{\tilde{\Pi}(i\zeta_l, y) + 2y(y^2 - \zeta_l^2)} \end{aligned} \quad (29)$$

and the dimensionless polarization tensor is given by

$$\begin{aligned} \tilde{\Pi}_{mn} &= \frac{2a}{\hbar} \Pi_{mn}, \\ \tilde{\Pi} &= \frac{8a^3}{\hbar} \Pi = (y^2 - \zeta_l^2)\tilde{\Pi}_{\text{tr}} - y^2\tilde{\Pi}_{00}. \end{aligned} \quad (30)$$

In terms of the variables (27), the dimensionless polarization tensor at zero temperature (4) is equal to

$$\begin{aligned} \tilde{\Pi}_{00}(i\zeta_l, y) &= \frac{\pi\alpha(y^2 - \zeta_l^2)}{f_l}, \\ \tilde{\Pi}(i\zeta_l, y) &= \pi\alpha(y^2 - \zeta_l^2)f_l, \end{aligned} \quad (31)$$

where

$$f_l \equiv f_l(y) = [\tilde{v}_F^2 y^2 + (1 - \tilde{v}_F^2)\zeta_l^2]^{1/2} \quad (32)$$

and $\tilde{v}_F \equiv v_F/c$ is the dimensionless Fermi velocity. The respective reflection coefficients at $T = 0$ K (where continuous frequency is replaced with discrete Matsubara frequencies) are obtained from Eq. (29)

$$\begin{aligned} r_{\text{TM}}^{(0)}(i\zeta_l, y) &= \frac{\pi\alpha y}{\pi\alpha y + 2f_l}, \\ r_{\text{TE}}^{(0)}(i\zeta_l, y) &= -\frac{\pi\alpha f_l}{\pi\alpha f_l + 2y}. \end{aligned} \quad (33)$$

The dimensionless thermal correction to the polarization tensor (31) is easily obtained from Eq. (10)

$$\begin{aligned}
\Delta_T \tilde{\Pi}_{00}(i\zeta_l, y) &= \frac{8\alpha f_l}{\tilde{v}_F^2} \int_0^\infty \frac{u}{e^{B_l u} + 1} \\
&\times \left\{ 1 - \frac{1}{\sqrt{2}} \left[\sqrt{(1+u^2)^2 - 4 \frac{\tilde{v}_F^2 (y^2 - \zeta_l^2) u^2}{f_l^2}} + 1 - u^2 \right]^{1/2} \right\}, \\
\Delta_T \tilde{\Pi}(i\zeta_l, y) &= \frac{8\alpha f_l}{\tilde{v}_F^2} \int_0^\infty \frac{du}{e^{B_l u} + 1} \\
&\times \left\{ -\zeta_l^2 + \frac{f_l^2}{\sqrt{2}} \left[\sqrt{(1+u^2)^2 - 4 \frac{\tilde{v}_F^2 (y^2 - \zeta_l^2) u^2}{f_l^2}} + 1 - u^2 \right]^{1/2} \right. \\
&\times \left. \left[1 - \frac{\tilde{v}_F^2 (y^2 - \zeta_l^2)}{f_l^2 \sqrt{(1+u^2)^2 - 4 \frac{\tilde{v}_F^2 (y^2 - \zeta_l^2) u^2}{f_l^2}}} \right] \right\},
\end{aligned} \tag{34}$$

where $B_l = \pi f_l / \tau$ and $\tau \equiv 4\pi a k_B T / (\hbar c)$ is dimensionless temperature.

Using Eqs. (12) and (31), we find approximate expressions for the polarization tensor in terms of dimensionless variables which are valid at all nonzero Matsubara frequencies

$$\begin{aligned}
\tilde{\Pi}_{00}(i\zeta_l, y) &= \frac{\alpha(y^2 - \zeta_l^2)}{f_l} (\pi + Y_l), \\
\tilde{\Pi}(i\zeta_l, y) &= \alpha(y^2 - \zeta_l^2) f_l (\pi + Y_l),
\end{aligned} \tag{35}$$

where Y_l is given by Eq. (13). The respective approximate reflection coefficients (15) valid at $l \geq 1$ take the form

$$\begin{aligned}
r_{\text{TM}}(i\zeta_l, y) &= \frac{\alpha y (\pi + Y_l)}{\alpha y (\pi + Y_l) + 2f_l}, \\
r_{\text{TE}}(i\zeta_l, y) &= -\frac{\alpha f_l (\pi + Y_l)}{\alpha f_l (\pi + Y_l) + 2y}.
\end{aligned} \tag{36}$$

Finally, the exact reflection coefficients (20) and (24) valid at zero Matsubara frequency in terms of dimensionless variables are given by

$$\begin{aligned}
r_{\text{TM}}(0, y) &= 1 - \frac{2\pi \tilde{v}_F^2 y}{\alpha \{8\tau \ln 2 + \pi \tilde{v}_F y [\pi - 8X(y)]\} + 2\pi \tilde{v}_F^2 y}, \\
r_{\text{TE}}(0, y) &= -\frac{\alpha \tilde{v}_F [\pi - 8Z(y)]}{\alpha \tilde{v}_F [\pi - 8Z(y)] + 2},
\end{aligned} \tag{37}$$

where the quantities $X(y)$ and $Z(y)$ are defined in Eqs. (19) and (23) taking into account that $B_0 = \pi \tilde{v}_F y / \tau$.

Now we are in a position to determine the accuracy of our approximate expressions and to investigate the origin of large thermal effect in the Casimir free energy between two graphene sheets at short separations. For this purpose we calculate the Casimir free energy (28) per unit area of two graphene sheets in three different ways. First, we compute the exact free energy $\mathcal{F}(a, T)$ using Eqs. (28) and (29), where the polarization tensor is given by the sum of respective expressions in Eqs. (31) and (34). Then, we perform calculations of the approximate free energy $\mathcal{F}^{(1)}(a, T)$ by using the exact reflection coefficients (37) at $\zeta_0 = 0$ and our asymptotic reflection coefficients (36) at all ζ_l with $l \geq 1$. Finally, we calculate the free energy $\mathcal{F}^{(2)}(a, T)$ using the approach of Ref. [18], i.e., by using the exact reflection coefficients (37) at $\zeta_0 = 0$ and coefficients (33) at all $l \geq 1$. Note that the approximate free energy $\mathcal{F}^{(1)}(a, T)$ takes an exact account of the explicit temperature dependence of the polarization tensor in the zero-frequency term of the Lifshitz formula. In all terms with $l \geq 1$ the explicit temperature dependence is taken into account approximately using our asymptotic approach. The approximate free energy $\mathcal{F}^{(2)}(a, T)$ takes into account an explicit temperature dependence only in the zero-frequency term and discards it in all terms with $l \geq 1$.

To compare the accuracies of both approximate calculation approaches, in Fig. 1(a) we plot the quantity

$$\delta\mathcal{F}^{(k)}(a, T) = \frac{\mathcal{F}(a, T) - \mathcal{F}^{(k)}(a, T)}{\mathcal{F}(a, T)} \quad (38)$$

at $T = 300$ K as a function of separation by the lines 1 and 2 in the region from $a = 5$ to 250 nm ($k = 1, 2$) for the first and second approaches, respectively. As is seen in Fig. 1(a) (line 1), the error of our asymptotic approach is negative and the maximum of its magnitude equal to 0.17% is achieved at the shortest separation $a = 5$ nm. With increase of separation to 10 and 30 nm the error magnitude decreases to 0.12% and 0.02%, respectively. At separations $a \geq 35$ nm our calculation approach becomes practically exact.

Note that the characteristic value of y giving the major contribution to the Casimir free energy (28) is $y = 1$. Taking this into account, the inequality (11) reduces to $\tau \gg \tilde{v}_F$. This inequality determines the region of separations and temperatures where our asymptotic approach is applicable for calculations of the Casimir free energy and pressure (for the latter see Sec. IV) in the framework of the Lifshitz theory. According to the results of Sec. II, at $T = 300$ K it should work well at $a \geq 10$ nm, where the parameter (11) is less than 0.17. From Fig. 1(a) (line 1) it is seen that the proposed asymptotic approach leads to rather

accurate result even at $a = 5$ nm where the parameter (11) is equal to 0.6. One should take into account, however, that the Dirac model of graphene is only applicable at energies below a few eV. This questions the possibility of using it for theoretical description of the Casimir force at separations below approximately 20 or even 30 nm [32].

The second approximate way of calculations turned out to be less accurate than the first one. As is seen from line 2 in Fig. 1(a), in this case the calculation error is positive. It is equal to 0.36% at $a = 5$ nm, achieves the largest value of 0.78% at $a = 20$ nm and then decreases to 0.49%, 0.21%, and 0.05% at separations 50, 100, and 250 nm, respectively. Taking into account, however, that in the second way of calculations the error remains to be below 1%, we conclude that the major contribution of an explicit temperature dependence of the polarization tensor to the Casimir effect originates from the zero-frequency Matsubara term.

Now we discuss an origin and sources of the large thermal effect in the Casimir free energy arising for graphene at short separations [8, 18, 20, 22]. For this purpose in Fig. 2(a) we plot the magnitudes of the Casimir free energy normalized to the quantity $A = k_B T / (8\pi a^2)$ at $T = 300$ K [see Eq. (28)] as functions of separation in the region from 5 to 250 nm. The upper line (\mathcal{F}) was computed at $T = 300$ K using the Lifshitz formula (28) and the reflection coefficients (29) with the exact polarization tensor defined as a sum of respective expressions in Eqs. (31) and (34). The nearly coinciding line [$\mathcal{F} = \mathcal{F}^{(1)}$] is obtained also by using our asymptotic reflection coefficients (36) at $l \geq 1$ and (37) at $l = 0$. The intermediate line [$\mathcal{F}^{(0)}$] was computed at $T = 300$ K using the Lifshitz formula (28) and the reflection coefficients (33), i.e., using the polarization tensor at $T = 0$, where continuous frequency was replaced by the discrete Matsubara frequencies. In this case an explicit dependence of the polarization tensor on T was discarded. Finally, the lowest line (\mathcal{F}_0) presents the Casimir free energy at $T = 0$ (i.e., the Casimir energy $E(a)$ per unit area of two graphene sheets) which, by definition, does not contain any thermal effect, either explicit or implicit.

As can be seen in Fig. 2(a), there is large implicit thermal effect for two graphene sheets at short separations due to a summation over the discrete frequencies. The magnitude of this effect is characterized by the difference between the intermediate and lowest lines [for better visualization in Fig. 2(b) the region from 5 to 30 nm is shown separately on an enlarged scale]. The difference between the upper and intermediate lines characterizes the magnitude of the explicit thermal effect arising from the dependence of the polarization tensor on the

temperature as a parameter [see also Fig. 2(b) at shorter separations]. As to the difference between the upper and lowest lines, it represents the total thermal correction to the Casimir energy. As is seen in Fig. 2, at moderate separations the explicit and implicit contributions to the thermal effect are nearly equal.

In Table I we illustrate the quantitative relationships between different constituent parts of the thermal correction and the role of the total thermal correction in the Casimir free energy at $T = 300$ K. In columns 2, 3, and 4 the fractions of explicit, $(|\mathcal{F}| - |\mathcal{F}^{(0)}|)/|\mathcal{F}|$, implicit, $(|\mathcal{F}^{(0)}| - |\mathcal{F}_0|)/|\mathcal{F}|$, and total $(|\mathcal{F}| - |\mathcal{F}_0|)/|\mathcal{F}|$, thermal corrections are presented at different separations indicated in column 1. The quantities $|\mathcal{F}|$, $|\mathcal{F}^{(0)}|$ and $|\mathcal{F}_0| = |E|$ are those plotted by the upper, intermediate and lowest lines in Fig. 2, respectively. As is seen in Table I (column 4), the thermal effect in graphene quickly increases with increase of separation and provides more than 80% contribution to the magnitude of the Casimir free energy at separations above 100 nm. In so doing at separations below 200 nm the TM mode contributes more than 99% of the free energy and more than 99.9% at $a > 200$ nm. An explicit thermal effect (column 2) contributes more than one half of the thermal correction at separations below 155 nm and at larger separations becomes less than an implicit thermal effect. However, our calculations show, that the magnitudes of both effects are similar and, thus, both of them must be taken into account in computations. We note also the role of the Matsubara term with $l = 0$. At separation distances of 30, 100, 200, and 1000 nm it contributes 69.3%, 94.4%, 98.4%, and 99.94% of the Casimir free energy, respectively.

As was mentioned in Sec. I, the thermal effect in the Casimir force for graphene becomes dominant at much shorter separations than for plates made of metallic or dielectric materials. For example, for ideal metal plates the relative thermal correction to the Casimir free energy at $T = 300$ K is equal to $(|\mathcal{F}| - |\mathcal{F}_0|)/|\mathcal{F}| = 3 \times 10^{-5}$ and 2.6×10^{-2} at separation distances $a = 100$ and 1000 nm, respectively. This should be compared with Table I, where the respective relative thermal effects for graphene are indicated as 0.7922 and 0.9788, i.e., by the factors of 2.6×10^5 and 37.6 larger.

The physical reason for such a big difference between graphene and other materials is the following. For ordinary metals and dielectrics the thermal effect becomes dominant when the contribution of all Matsubara terms with $l \geq 1$ becomes exponentially small due to the exponential factors in Eq. (26). At $T = 300$ K this happens at separations above 5 or 6 μm . In doing so, the remaining zero-frequency Matsubara term alone describes

the classical thermal Casimir effect. As to graphene, at short separations above 100 nm, where the exponential factors in Eq. (26) are not small yet, the reflection coefficients in all Matsubara terms with $l \geq 1$ become very small making dominant the classical thermal contribution of the zero-frequency term.

IV. INVESTIGATION OF THE THERMAL EFFECT FOR THE CASIMIR PRESSURE

The Lifshitz formula for the Casimir pressure between two parallel graphene sheets is given by [3, 4, 16]

$$P(a, T) = -\frac{k_B T}{\pi} \sum_{l=0}^{\infty}{}' \int_0^{\infty} q_l k_{\perp} dk_{\perp} \{ [r_{\text{TM}}^{-2}(i\xi_l, k_{\perp}) e^{2aq_l} - 1]^{-1} + [r_{\text{TE}}^{-2}(i\xi_l, k_{\perp}) e^{2aq_l} - 1]^{-1} \}, \quad (39)$$

where the exact reflection coefficients are written in Eq. (1) with the polarization tensor presented in Eqs. (3), (4) and (7).

In terms of the dimensionless variables (27) convenient in numerical computations Eq. (39) takes the form

$$P(a, T) = -\frac{k_B T}{8\pi a^3} \sum_{l=0}^{\infty}{}' \int_{\zeta_l}^{\infty} y^2 dy \{ [r_{\text{TM}}^{-2}(i\zeta_l, y) e^y - 1]^{-1} + [r_{\text{TE}}^{-2}(i\zeta_l, y) e^y - 1]^{-1} \}, \quad (40)$$

where the exact reflection coefficients can be found in Eq. (29) and the dimensionless polarization tensor is presented in Eqs. (31) and (34). The approximate reflection coefficients at all nonzero Matsubara frequencies ($l \geq 1$) using our asymptotic approach are given in Eq. (36). At zero Matsubara frequency the exact reflection coefficients are written in Eq. (37).

First, we determine the accuracy of our approximate method in application to calculations of the Casimir pressure. To do this, we calculate the Casimir pressure (40) in three different ways already discussed in Sec. III. As a result, we obtain the exact Casimir pressure $P(a, T)$, the approximate Casimir pressure $P^{(1)}(a, T)$ computed using our asymptotic approach and the approximate pressure $P^{(2)}(a, T)$ using the approach of Ref. [18] discarding an explicit dependence of the polarization tensor on T in Matsubara terms with $l \geq 1$. The accuracies

of both approximate methods are characterized by the quantities

$$\delta P^{(k)}(a, T) = \frac{P(a, T) - P^{(k)}(a, T)}{P(a, T)}. \quad (41)$$

In Fig. 1(b) we plot the quantities $\delta P^{(1)}$ and $\delta P^{(2)}$ at $T = 300$ K as a function of separation by the lines 1 and 2, respectively. As is seen in Fig. 1(b) (line 1), the error of our asymptotic approach in calculations of the Casimir pressure is negative and the maximum of its magnitude is equal to 0.18% at $a = 5$ nm. At separations of 10 and 30 nm the error magnitude decreases to 0.16% and 0.01%, respectively, and becomes nearly zero at $a \geq 35$ nm.

For the second approximate way of calculations [the line 2 in Fig. 1(b)] the error is positive. It is equal to 0.22% at $a = 5$ nm, achieves the largest value of 0.87% at $a = 30$ nm and then decreases to 0.69%, 0.35%, and 0.09% at separations 50, 100, and 250 nm, respectively. Thus, our asymptotic expressions for the polarization tensor of graphene and reflection coefficients lead to more exact results than the approximate method discarding an explicit temperature dependence of the polarization tensor at all $l \geq 1$. Nevertheless, the main contribution to the explicit thermal effect in the Casimir pressure, similar to the free energy, originates from the zero-frequency Matsubara term.

To investigate an origin and sources of the large thermal effect, in Fig. 3(a) we plot the magnitudes of the Casimir pressure normalized to the quantity $B = k_B T / (8\pi a^3)$ at $T = 300$ K [see Eq. (28)] as functions of separation. The upper, intermediate and lowest lines in Fig. 3(a,b) were obtained in the same ways as the respective lines in Fig. 2(a,b), i.e., the upper line [$P = P^{(1)}$] was computed at $T = 300$ K exactly by using Eqs. (29), (31), (34) and (40), the intermediate line [$P^{(0)}$] at $T = 300$ K by Eqs. (33) and (40), and the lowest line (P_0) is the Casimir pressure computed at $T = 0$.

From Fig. 3(a) it is seen that, similar to the free energy, there is large implicit thermal effect in the Casimir pressure between two graphene sheets at short separations, characterized by the difference between the intermediate and lowest lines. [The separation region from 5 to 30 nm is shown on an enlarged scale in Fig. 3(b).] The explicit thermal effect in the Casimir pressure is shown in Fig. 3(a,b) by the difference between the upper and intermediate lines. This contribution to the total thermal correction (the latter is shown by the difference between the upper and lowest lines) originates from the dependence of the polarization tensor on the temperature as a parameter. Again, at moderate separations the explicit and implicit thermal effects contribute to the total thermal correction nearly equal.

The quantitative results are listed in Table II. The first column of this table contains the values of separation and the columns 2, 3, and 4 the values of $(|P| - |P^{(0)}|)/|P|$, $(|P^{(0)}| - |P_0|)/|P|$, and $(|P| - |P_0|)/|P|$, where the magnitudes of the Casimir pressure $|P|$, $|P^{(0)}|$, and $|P_0|$ are the exact ones (the upper line), the ones computed at $T = 300$ K using the zero-temperature polarization tensor (the intermediate line), and the ones computed at $T = 0$ (the lowest line), respectively. Similar to the case of the free energy, the thermal effect in the Casimir pressure quickly increases with increase of separation (column 4). At separations above 150 nm the thermal effect contributes more than 80% of the Casimir pressure between two graphene sheets. The contribution of an explicit thermal effect in the Casimir pressure (column 2) is larger than that of an implicit at all separations below or equal 325 nm. At separation distances 30, 100, 200, and 1000 nm the zero-frequency Matsubara term contributes 55.7%, 89.9%, 96.9%, and 99.86% of the Casimir pressure, respectively. Similar to the case of the Casimir free energy, the thermal effect for the Casimir pressure becomes dominant at much shorter separations than for metallic and dielectric materials. Thus, for two ideal metal plates at separation distances $a = 100$ and 1000 nm one has $(|P| - |P_0|)/|P| = 1.57 \times 10^{-7}$ and 1.57×10^{-3} , respectively. From Table II we conclude that for graphene the relative thermal effect at the same respective separations is larger by the factors of 5.6×10^7 and 6.2×10^2 . As to the relative role of the TM and TE modes in the total Casimir pressure, the TM mode remains dominant and provides more than 99% of the pressure magnitude. In precise computations, however, both modes should be taken into account.

V. CONCLUSIONS AND DISCUSSION

In the foregoing we have obtained simple asymptotic expressions for the polarization tensor of graphene and reflection coefficients at nonzero Matsubara frequencies suitable for calculation of the Casimir free energy and pressure between two parallel graphene sheets. This has been made possible by applying the new form of the polarization tensor [33] valid not only at the imaginary Matsubara frequencies, but over the entire plane of complex frequency. In this paper, the analytic asymptotic expressions are derived by means of perturbation expressions in powers of a natural parameter which becomes small over the wide range of physically interesting separations and temperatures. The respective expressions for

the Casimir free energy and pressure between two graphene sheets take into account both an explicit dependence of the polarization tensor (or, equivalently, conductivity, or dielectric permittivity, or density-density correlation function) on the temperature as a parameter and an implicit temperature dependence through a summation over the Matsubara frequencies.

Using the obtained asymptotic expressions for the reflection coefficients, we have compared the Casimir free energy and pressure calculated in the framework of our formalism with the previously known ones [22] calculated numerically using the polarization tensor of Ref. [18]. It was shown that our asymptotic approach leads to very accurate results (the maximum errors are equal to 0.17% and 0.18% at the separation of 5 nm for the Casimir free energy and pressure, respectively). These errors decrease with increase of separation. At all separations above 35 nm the asymptotic Casimir free energies and pressures coincide with the exact ones.

We have investigated an origin of large thermal effect arising in the Casimir interaction between graphene sheets at short separations [8]. We have shown that the total thermal corrections to the Casimir energy and pressure at zero temperature consist of two parts. The explicit part is determined by the parametric dependence of the polarization tensor on T , whereas the implicit one arises through a summation over the Matsubara frequencies. According to our results, in both the Casimir free energy and pressure, an explicit thermal effect exceeds an implicit one at shorter separations. At moderate separations both parts of the thermal effect are similar in magnitudes. With further increase of separation an implicit thermal effect in the Casimir free energy and pressure becomes larger than an explicit one. We have also confirmed the previously known result [18, 22] that the thermal effect in the Casimir interaction between two graphene sheets contributes more than 80% of the Casimir free energy and pressure at relatively short separations exceeding 100 and 150 nm, respectively, and that the major contribution to both the free energy and pressure is given by the electromagnetic field with transverse magnetic polarization.

In future it would be interesting to extend our asymptotic approach to real frequency axis and obtain simple analytic expressions for the polarization tensor, conductivity, density-density correlation functions and dielectric permittivity of graphene at nonzero temperature for numerous applications other than the Casimir effect. As an example, one could mention

calculation of the reflectivity properties of graphene over a wide range of real frequencies.

-
- [1] M. I. Katsnelson, *Graphene: Carbon in Two Dimensions* (Cambridge University Press, Cambridge, 2012).
 - [2] A. H. Castro Neto, F. Guinea, N. M. R. Peres, K. S. Novoselov, and A. K. Geim, *Rev. Mod. Phys.* **81**, 109 (2009).
 - [3] V. A. Parsegian, *Van der Waals Forces: A Handbook for Biologists, Chemists, Engineers, and Physicists* (Cambridge University Press, Cambridge, 2005).
 - [4] M. Bordag, G. L. Klimchitskaya, U. Mohideen, and V. M. Mostepanenko, *Advances in the Casimir Effect* (Oxford University Press, Oxford, 2009).
 - [5] J. F. Dobson, A. White, and A. Rubio, *Phys. Rev. Lett.* **96**, 073201 (2006).
 - [6] M. Bordag, *J. Phys. A: Math. Gen.* **39**, 6173 (2006).
 - [7] M. Bordag, B. Geyer, G. L. Klimchitskaya, and V. M. Mostepanenko, *Phys. Rev. B* **74**, 205431 (2006).
 - [8] G. Gómez-Santos, *Phys. Rev. B* **80**, 245424 (2009).
 - [9] D. Drosdoff and L. M. Woods, *Phys. Rev. B* **82**, 155459 (2010).
 - [10] D. Drosdoff and L. M. Woods, *Phys. Rev. A* **84**, 062501 (2011).
 - [11] T. E. Judd, R. G. Scott, A. M. Martin, B. Kaczmarek, and T. M. Fromhold, *New. J. Phys.* **13**, 083020 (2011).
 - [12] Bo E. Sernelius, *Europhys. Lett.* **95**, 57003 (2011).
 - [13] V. Svetovoy, Z. Moktadir, M. Elvenspoek, and H. Mizuta, *Europhys. Lett.* **96**, 14006 (2011).
 - [14] Bo E. Sernelius, *Phys. Rev. B* **85**, 195427 (2012).
 - [15] A. D. Phan, L. M. Woods, D. Drosdoff, I. V. Bondarev, and N. A. Viet, *Appl. Phys. Lett.* **101**, 113118 (2012).
 - [16] E. M. Lifshitz and L. P. Pitaevskii, *Statistical Physics, Part II* (Pergamon, Oxford, 1980).
 - [17] M. Bordag, I. V. Fialkovsky, D. M. Gitman, and D. V. Vassilevich, *Phys. Rev. B* **80**, 245406 (2009).
 - [18] I. V. Fialkovsky, V. N. Marachevsky, and D. V. Vassilevich, *Phys. Rev. B* **84**, 035446 (2011).
 - [19] Yu. V. Churkin, A. B. Fedortsov, G. L. Klimchitskaya, and V. A. Yurova, *Phys. Rev. B* **82**, 165433 (2010).

- [20] M. Bordag, G. L. Klimchitskaya, and V. M. Mostepanenko, Phys. Rev. B **86**, 165429 (2012).
- [21] M. Chaichian, G. L. Klimchitskaya, V. M. Mostepanenko, and A. Tureanu, Phys. Rev. A **86**, 012515 (2012).
- [22] G. L. Klimchitskaya and V. M. Mostepanenko, Phys. Rev. B **87**, 075439 (2013).
- [23] G. L. Klimchitskaya and V. M. Mostepanenko, Phys. Rev. B **89**, 035407 (2014).
- [24] G. L. Klimchitskaya and V. M. Mostepanenko, Phys. Rev. A **89**, 012516 (2014).
- [25] G. L. Klimchitskaya and V. M. Mostepanenko, Phys. Rev. A **89**, 062508 (2014).
- [26] B. Arora, H. Kaur, and B. K. Sahoo, J. Phys. B **47**, 155002 (2014).
- [27] K. Kaur, J. Kaur, B. Arora, and B. K. Sahoo, Phys. Rev. B **90**, 245405 (2014).
- [28] G. L. Klimchitskaya, V. M. Mostepanenko, and Bo E. Sernelius, Phys. Rev. B **89**, 125407 (2014).
- [29] G. L. Klimchitskaya, U. Mohideen, and V. M. Mostepanenko, Phys. Rev. B **89**, 115419 (2014).
- [30] G. L. Klimchitskaya and V. M. Mostepanenko, Phys. Rev. A **89**, 052512 (2014).
- [31] A. A. Banishev, H. Wen, J. Xu, R. K. Kawakami, G. L. Klimchitskaya, V. M. Mostepanenko, and U. Mohideen, Phys. Rev. B **87**, 205433 (2013).
- [32] G. L. Klimchitskaya and V. M. Mostepanenko, Phys. Rev. A **91**, 045412 (2015).
- [33] M. Bordag, G. L. Klimchitskaya, V. M. Mostepanenko, and V. M. Petrov, Phys. Rev. D **91**, 045037 (2015).
- [34] G. L. Klimchitskaya, U. Mohideen, and V. M. Mostepanenko, Rev. Mod. Phys. **81**, 1827 (2009).

TABLE I: Different constituent parts of the relative thermal correction to the Casimir free energy (column 4) arising (column 2) from an explicit dependence of the polarization tensor on temperature and (column 3) from an implicit temperature dependence through a summation over the Matsubara frequencies are shown at $T = 300$ K at different separations between two graphene sheets (column 1). See text for further discussion.

a (nm)	$\frac{ \mathcal{F} - \mathcal{F}^{(0)} }{ \mathcal{F} }$	$\frac{ \mathcal{F}^{(0)} - \mathcal{F}_0 }{ \mathcal{F} }$	$\frac{ \mathcal{F} - \mathcal{F}_0 }{ \mathcal{F} }$
5	0.0312	0.0082	0.0394
10	0.0922	0.0347	0.1269
20	0.2013	0.1068	0.3081
30	0.2730	0.1734	0.4464
50	0.3492	0.2680	0.6172
100	0.4115	0.3807	0.7922
150	0.4303	0.4289	0.8592
200	0.4387	0.4552	0.8939
250	0.4432	0.4717	0.9149
500	0.4511	0.5064	0.9575
1000	0.4543	0.5245	0.9788

TABLE II: Different constituent parts of the relative thermal correction to the Casimir pressure (column 4) arising (column 2) from an explicit dependence of the polarization tensor on temperature and (column 3) from an implicit temperature dependence through a summation over the Matsubara frequencies are shown at $T = 300$ K at different separations between two graphene sheets (column 1). See text for further discussion.

a (nm)	$\frac{ P - P^{(0)} }{ P }$	$\frac{ P^{(0)} - P_0 }{ P }$	$\frac{ P - P_0 }{ P }$
5	0.0144	0.0019	0.0163
10	0.0506	0.0123	0.0619
20	0.1365	0.0493	0.1858
30	0.2086	0.0967	0.3053
50	0.3014	0.1822	0.4836
100	0.3928	0.3096	0.7024
150	0.4234	0.3716	0.7950
200	0.4374	0.4072	0.8446
250	0.4452	0.4300	0.8752
500	0.4584	0.4790	0.9374
1000	0.4637	0.5051	0.9688

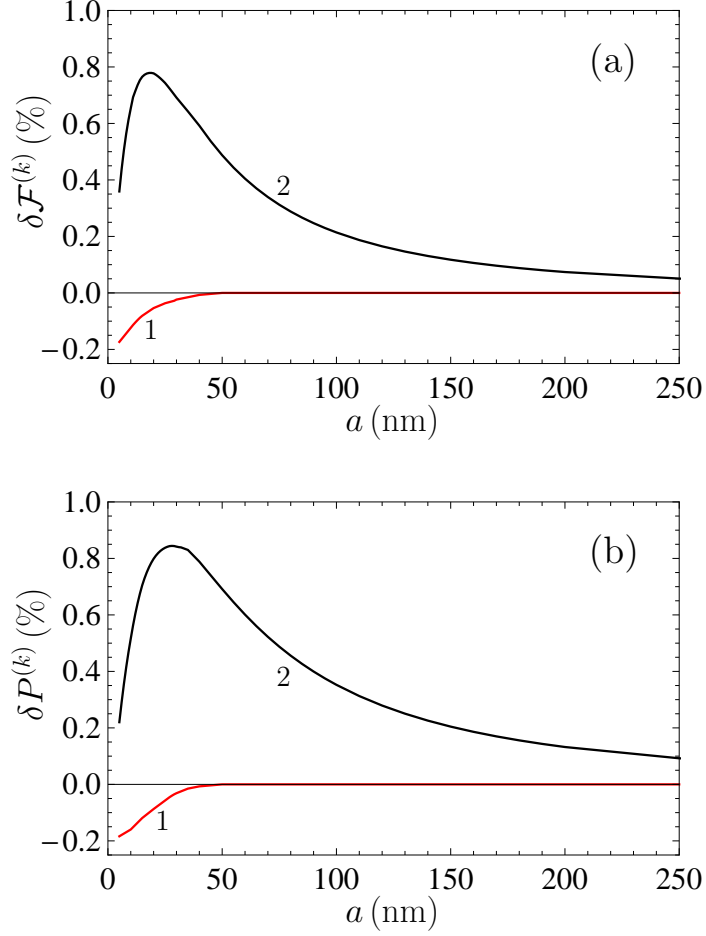


FIG. 1: (Color online) The relative errors of the approximate methods for calculation of the Casimir (a) free energy and (b) pressure between two graphene sheets using (line 1) our asymptotic approach taking into account an explicit temperature dependence of the polarization tensor in all Matsubara terms and (line 2) discarding this dependence in terms with $l \geq 1$ are shown as functions of separation.

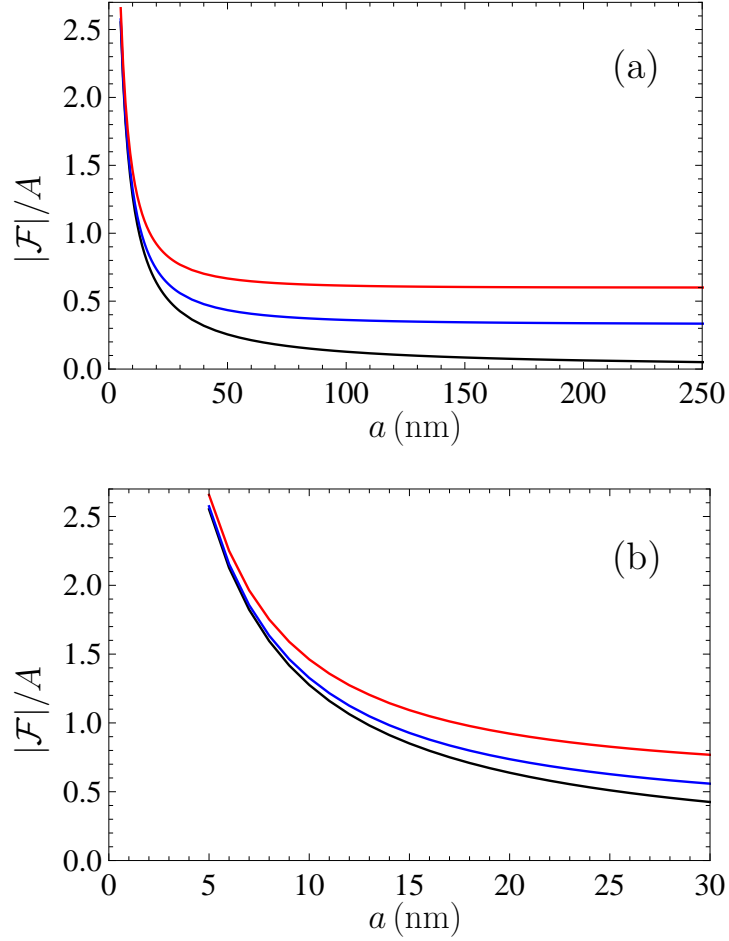


FIG. 2: (Color online) The normalized Casimir free energy per unit area of two graphene sheets at $T = 300$ K calculated (the upper line) exactly and (the intermediate line) taking into account only an implicit temperature dependence through a summation over the Matsubara frequencies are shown as functions of separation. The normalized Casimir energy at zero temperature is presented as a function of separation by the lowest line.

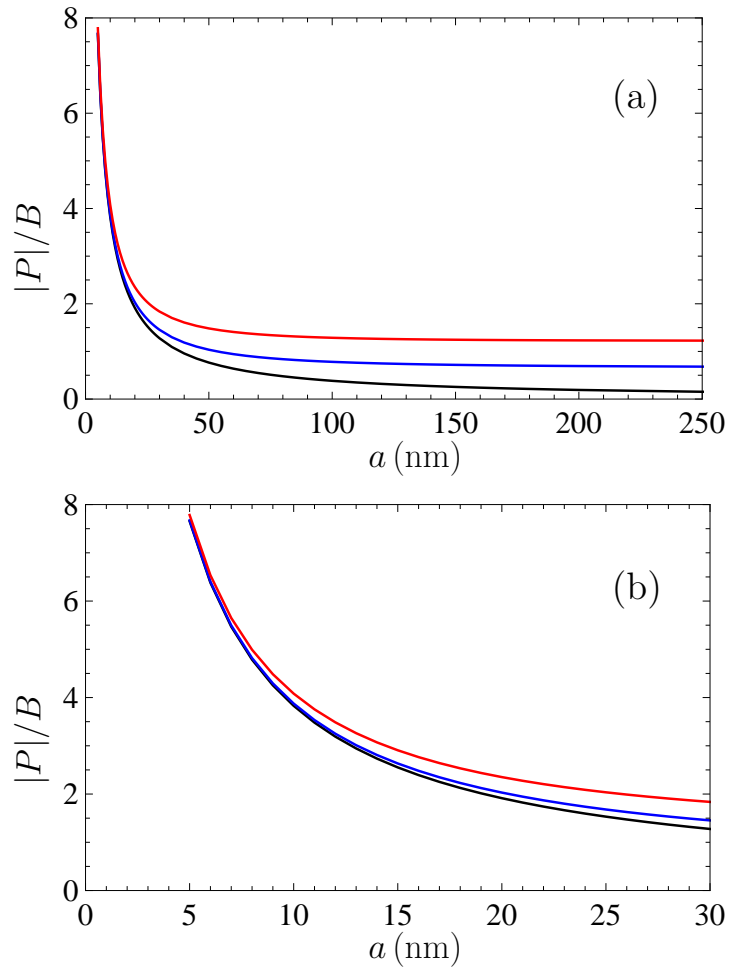


FIG. 3: (Color online) The normalized Casimir pressure between two graphene sheets at $T = 300$ K calculated (the upper line) exactly and (the intermediate line) taking into account only an implicit temperature dependence through a summation over the Matsubara frequencies are shown as functions of separation. The normalized Casimir pressure at zero temperature is presented as a function of separation by the lowest line.